ISBN: 978-3-95450-205-9 doi:10.18429/JACoW-Cyclotrons2019-FRB03

3D RADIO FREQUENCY SIMULATION OF THE INFN-LNS SUPERCONDUCTING CYCLOTRON

G. Torrisi*, L. Neri, L. Allegra, L. Calabretta, A. Caruso, G. Costa,
G. Gallo, A. Longhitano, D. Rifuggiato
INFN-LNS, Catania, Italy

Abstract

An upgrade plan of the Superconducting Cyclotron operating at INFN-LNS is ongoing. In this paper, a 3D numerical model of the Cyclotron radio frequency cavity is presented. Simulations include the coaxial sliding shorts, liner vacuum chamber, coupler, trimming capacitor and the Dees structures. CST microwave studio software has been used for numerical computation. RF simulations are mandatory also in order to analyze the field in the beam region and evaluate the impact of different Dees geometry and eventual field asymmetries. Moreover, 3D COMSOL Multiphysics simulations have been carried out in order to couple the electromagnetic field solution to a custom beam-dynamics code developed in Matlab as a future plan. Time evolution of accelerated beam and electromagnetic field make also possible to verify the magnetic field synchronization. Experimental validation of the developed model will be also presented.

INTRODUCTION

The INFN-LNS Superconducting Cyclotron (SC) is a three sector compact machine with a wide operating range, able to accelerate heavy ions with values of q/A from 0.1 to 0.5 to energy from 2 to 100 AMeV [1]. The SC has been in operation for more than 20 years for nuclear physics experiments, which require low intensity beams. Up to now the maximum beam power has been limited to 100 W due to the beam dissipation on the electrostatic deflectors. To fulfill the request of users aiming to study rare processes in Nuclear Physics [2, 3], the beam power has to be increased up to 2-10 kW for ions with mass lower than 40 a.m.u., and extracted by stripping [4–6]. The feasibility of extraction by stripping through an optimized extraction channel with an increased transverse section has been studied in [7–9]. In the meantime, the RF system has gone through many improvements for more reliable operation of the cyclotron [10, 11]. Moreover, the vertical gap between the dees of the acceleration chamber is planned to be increased from the present 24 mm up to 30 mm by renewing the existing liners and trim coils [12]. This paper describes a numerical study of the RF cavity of the INFN-LNS SC, especially focused on the eventual vertical asymmetry at the dee gap. RF driven-field simulations allow to investigate the fundamental accelerating mode and eventual RF leakages and asymmetries [13–16].

* giuseppe.torrisi@lns.infn.it

RF NUMERICAL MODEL VS EXPERIMENTAL RESULTS

The 3D model was created by using Autodesk Inventor [17] to provide a proper geometry with the actual dimensions to the 3D commercial electromagnetic simulators, CST Microwave Studio [18] and COMSOL multiphysics [19]. In particular, COMSOL could be used connected to a MATLAB-developed beam dynamics code [8]. In Fig. 1 the overall geometry of the simulated model of RF cavity of the LNS SC it is shown: the dee stems, the trimmer, the coupler and the dees have been included into the simulation. Figure 2 shows the CST MWS simulated 3D Electric field distribution vector (left) and intensity (right). The RF Cavity has a

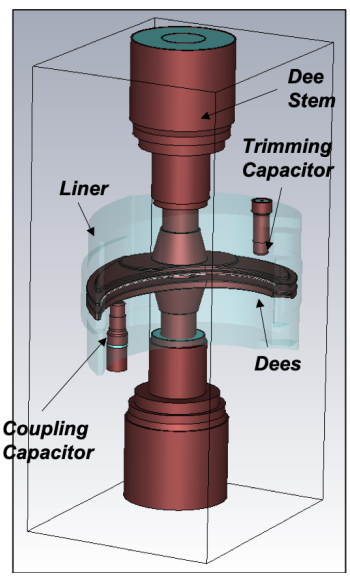

Figure 1: Overall geometry of the simulated model of RF cavity of the LNS Superconducting Cyclotron (SC).

capacitive coupled power input, while, on the other side of cyclotron, cavity has a tuner. Both the components are controlled by external motor for tuning of the cavity matching and frequency. For COMSOL simulations (see Fig. 3), we added an external lateral volume in correspondence of the dee plane to the previous geometry, in order to simulate the "accelerating" electric field for the beam-dynamics code.

As experimental validation of the developed model we performed driven RF simulation by varying the coupler and trimmer position. Figure 4 shows that a good impedance matching (in terms of $|S_{11}|$) can be obtained by moving the coupler towards the dee-plane. The comparison between the numerical results of Fig. 4 and the experimental results

ISBN: 978-3-95450-205-9 doi:10.18429/JACoW-Cyclotrons2019-FRB03

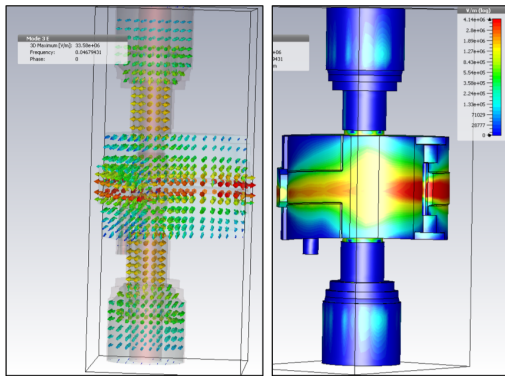

Figure 2: CST MWS simulated 3D Electric field distribution vector (left) and intensity (right).

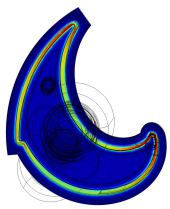

Figure 3: COMSOL Numerical simulation result: Electric field norm on the median dee-plane.

of Fig. 5 confirms also that the tuner positioning allow a fine-tuning of the resonant frequency. The RF scattering parameters have been computed and are in agreement with the parameters measured on the cyclotron: both in simulation (Fig. 4) and measurement (Fig. 5), we can observe a frequency downshift of the resonant frequency by moving the coupler from the initial position ("c=start") towards the median plane ("c=+30 mm" in simulation, "c=+25 mm and c=+50 mm" in measurements).

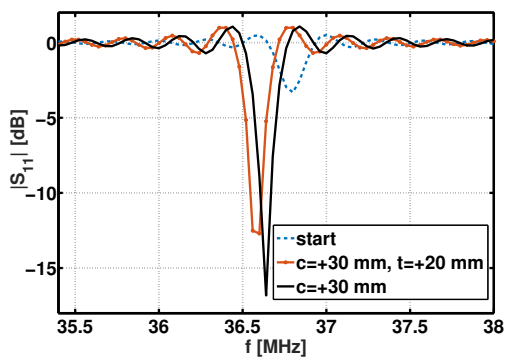

Figure 4: CST MWS Numerical simulation results: Comparison of the reflection coefficient $|S_{11}|$ for three different configurations obtained by varying the coupler and the trimmer vertical positions ("c" and "t" in the legend). In the legend, "start" indicates that coupler and trimmer have a distance from the dee-plane of 146 mm. The sign "+" means to get closer to the dee-plane with respect to the "start" position.

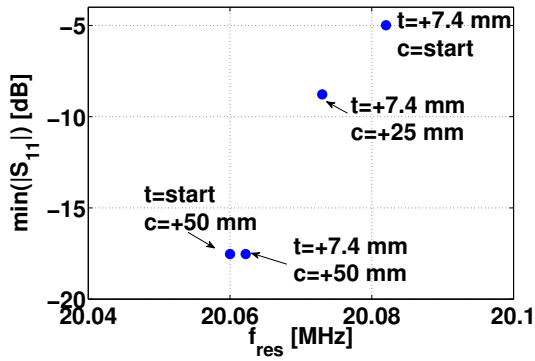

Figure 5: Measured results with Network analyzer: Comparison of the minimum reflection coefficient ($\min(|S_{11}|)$) for different configurations obtained by varying the coupler and the trimmer vertical positions ("c" and "t" in the legend).

ELECTROMAGNETIC STUDY OF DEES ASYMMETRY

Due to the different size of the beam for the SC upgrade plan [5], the vertical gap between the dees has to be increased from 25 to 31 mm, 6 mm of difference, 3 mm up and 3 mm down. This modification results in the length reduction of the conical connection between the stem (inner coaxial) and the dee (see the comparison of the "old" and "new" geometry in Fig 6).

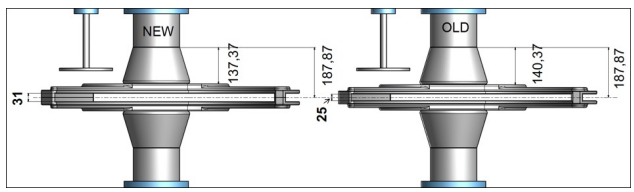

Figure 6: Comparison of the "old" and "new" geometry (sizes in mm-unit): the reduction of the length of the conical connection between the stem (inner coaxial) and the dee from 140.37 mm (on the right) to 137.37 mm (on the left) increases the dee vertical gap size Δg from 24 to 30 mm in the "new geometry".

Using the CST Microwave Studio, we checked the proposed length reduction, of ± 3 mm (up and down), of the conical connection (dee-inner coax), can be accepted, in terms of maximum electric field distribution, around the critical zone of the nose, electric field along the vertical axis (see Fig. 7) and no parasitic modes appear. In order to host the new stripping extraction system, a new dee geometry has been proposed. In this Section, we evaluate the impact of the different dee geometry on the electric field distribution on the medium plane using the CST Microwave Studio. For the simulations, three models were created: the actual geometry (Fig. 8 (a)) used as a reference for RF simulations preserving the actual cavity structure; a second asymmetric model (Fig. 8 (b)) with the top actual dee and the new bottom; a third model where both the dees have the new geometry (Fig. 8 (c)). In order to explore the eventual presence of parasitic

ISBN: 978-3-95450-205-9 doi:10.18429/JACoW-Cyclotrons2019-FRB03

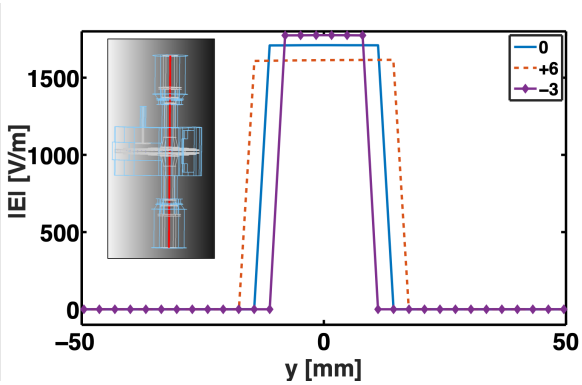

Figure 7: Norm of electric field along the vertical axis (red line in the inset) crossing the dee of the RF cavity for different values Δg of the vertical gap between the dees.

electric field components, the resulting electric field orthogonal to the medium (accelerating) plane is shown in Fig. 9 (plotted on the same plane). As we would expect, Fig. 9 (a) shows the unwanted electric field component is near zero in the first symmetric case (actual geometry, Fig. 8 (a)). On the other hand, the geometrical asymmetry of the second case (asymmetric model Fig. 8 (b)) gives rise to undesired electric field intensity (Fig. 9 (b)) in the central part of the dee medium plane. This undesired effect can be only partially avoided by using the third case geometry (Fig. 8 (c)): anyway, in this latter case, Fig. 9 (c) shows fringing field due to the "edge" effect ot the "new" dees.

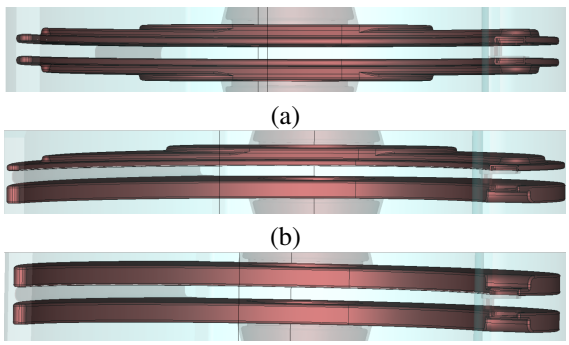

(a)

(b)

(c)

Figure 8: 3D view of the Dees geometry: a) current configuration. b) asymmetric configuration with the new dee; c) symmetric configuration with the new dees.

CONCLUSION

A better understanding of RF behavior in the SC was possible by using Electromagnetic 3D simulation. Close agreement between measured and computed S-parameters demonstrates the usefulness of the simulation. The full structure model of the cyclotron was used to study eventual asymmetry. This model simulation can be further used to study the center region of the accelerator, RF leakages, parasitic modes. 3D COMSOL Multiphysics simulations could be carried out in order to couple the electromagnetic field solution to a custom beam-dynamics code developed in Matlab as scope of future work.

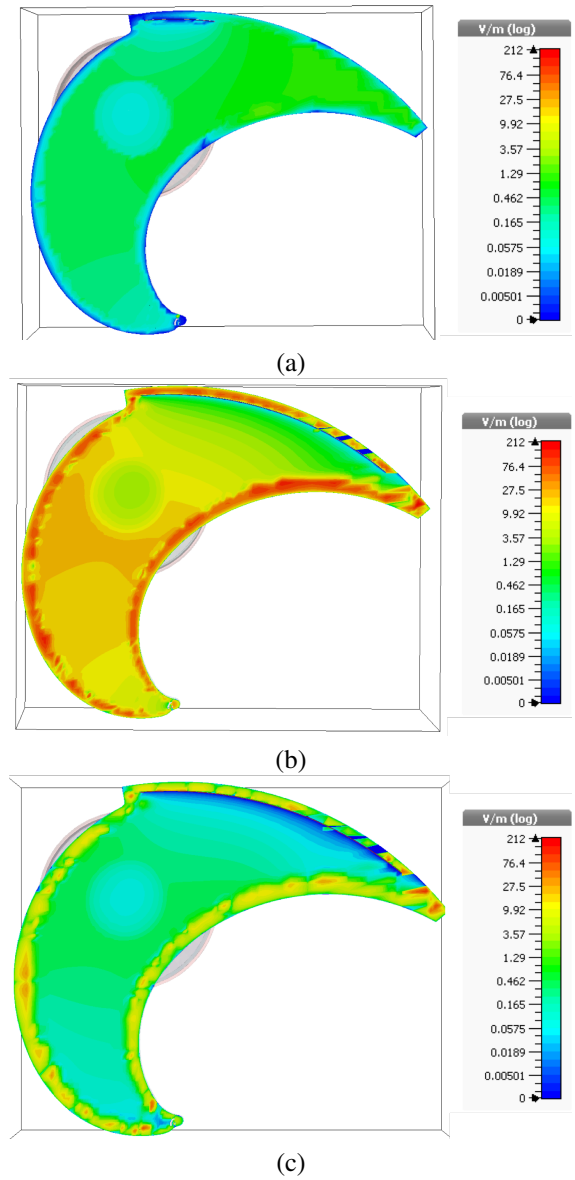

(a)

(b)

(c)

Figure 9: Cross Section view of the Electric field (same scale) for the three geometry: a) current configuration. b) asymmetric configuration with the new dee; c) symmetric configuration with the new dees

REFERENCES

[1] L. Calabretta *et al.*, "Commissioning of the K800 INFN Cyclotron," in *Proc. Cyclotrons'95*, Faure, Cape Town, South Africa, 8-13 Oct 1995, p. A02, 1996.

[2] F. Cappuzzello, F, M. Cavallaro, C. Agodi, M. Bondì, D. Carbone, A. Cunsolo, and A. Foti, "Heavy-ion double charge exchange reactions: A tool toward $0\nu\beta\beta$ nuclear matrix elements," *Eur. Phys. J. A*, vol. 51, no. 11, p. 145, 2015. doi:10.1140/epja/i2015-15145-5

[3] F. Cappuzzello *et al.*, "The NUMEN project: NUclear Matrix Elements for Neutrinoless double beta decay," *Eur. Phys. J. A*, vol. 54, no. 5, p. 72, 2018. doi:10.1140/epja/i2018-12509-3

[4] A. Calanna *et al.*, "Proposal to increase the extracted beam power from the LNS-INFN Superconducting Cyclotron," in

ISBN: 978-3-95450-205-9 doi:10.18429/JACoW-Cyclotrons2019-FRB03

Proc. HIAT2015, Yokohama, Japan, Sep. 2015, pp. 23–26. doi:10.18429/JACoW-HIAT2015-MOA1C03

[5] L. Calabretta, A. Calanna, G. Cuttone, G. D'Agostino, D. Rifuggiato, and A. D. Russo, "Upgrade of the LNS superconducting cyclotron for beam power higher than 2-5 kW," in *Proc. Cyclotrons'16*, Zurich, Switzerland, Sep. 2016, pp. 7–10. doi:10.18429/JACoW-Cyclotrons2016-MOA02

[6] A. Calanna, "High-intensity extraction from the Superconducting Cyclotron at LNS-INFN," *Nuovo Cimento C Geophysics Space Physics C*, vol. 40, p. 101, Mar. 2017. doi:10.1393/ncc/i2017-17101-y

[7] G. D'Agostino, L. Calabretta, W. J. G. M. Kleeven, and D. Rifuggiato, "A central region upgrade of the K800 Superconducting Cyclotron at INFN-LNS," in *Proc. IPAC'19*, Melbourne, Australia, May 2019, pp. 1975–1978. doi:10.18429/JACoW-IPAC2019-TUPTS023

[8] L. Neri, G. D'Agostino, L. Calabretta, D. Rifuggiato, A. Russo, and G. Torrisi, "3D Magnetic optimization of the new extraction channel for the LNS Superconducting Cyclotron," presented at the Cyclotrons'19, Cape Town, South Africa, Sep. 2019. doi:10.18429/JACoW-Cyclotrons2019-MOP014, to be published

[9] G. Gallo, G. Costa, L. Allegra, L. Calabretta, G. Messina, M. Musumeci, D. Rifuggiato, and E. Zappalà, "Mechanical modifications of the median plane for the Superconducting Cyclotron upgrade," presented at the Cyclotrons'19, Cape Town, South Africa, Sep. 2019. doi:10.18429/JACoW-Cyclotrons2019-MOP013, to be published

[10] A. Caruso, "The RF System of the K-800 Superconducting Cyclotron at INFN-LNS," in *Proc. InPAC'13*, Nov 2013, Kolkata, India, paper InPAC2013IT15.

[11] A. C. Caruso, F. Caruso, A. Longhitano, A. Spartà, G. Primadei, and J. Sura, "Hybrid configuration, solid state-tube, revamps an obsolete tube amplifier for the INFB K-800 Superconducting Cyclotron," in *Proc. Cyclotrons'16*, Zurich, Switzerland, Sep. 2016, pp. 263–266. doi:10.18429/JACoW-Cyclotrons2016-WEB02

[12] G. Gallo, L. Allegra, G. Costa, E. Messina, and E. Zappalà, "Mechanical aspects of the LNS Superconducting Cyclotron upgrade," in *Proc. Cyclotrons'16*, Zurich, Switzerland, Sep. 2016, paper THP09, pp. 322–324. doi:10.18429/JACoW-Cyclotrons2016-THP09

[13] J. J. Livingood, *Principles of Cyclic Particle Accelerators*, London: D. van Nostrand Co, 1961.

[14] V. Afzalan, H. Afarideh, R. Azizi, M. Ghergherehchi, and J. S. Chai, "Design and simulation of cavity for 10 MeV compact cyclotron," in *Proc. Cyclotrons'13*, Vancouver, Canada, Sep. 2013, paper TUPPT023, pp. 200–202.

[15] A. K. Mitra, Y. Bylinski, N. Mehboob, R. L. Poirier, and V. Zvyagintsev, "Simulation of RF structure of TRIUMF cyclotron with HFSS," in *Proc. Cyclotrons'04*, Tokyo, Japan, Oct. 2004, paper 20P29, pp. 365-367.

[16] M. Mohamadian, H. Afarideh, M. Ghergherehchi, S. Sabounchi, and M. Salehi, "Equivalent circuit model of cyclotron rf system," in *Proc. Cyclotrons'16*, Zurich, Switzerland, Sep. 2016, pp. 39–41. doi:10.18429/JACoW-Cyclotrons2016-MODM03

[17] Autodesk, "Autodesk Inventor."

[18] CST, "CST Microwave Studio," 2017.

[19] "Comsol Multiphysics reference manual, version 5.3.